



Article

# Monitoring of Cropland Abandonment Based on Long Time Series Remote Sensing Data: A Case Study of Fujian Province, China

**Jiayu Wu** <sup>1</sup>, **Shaofei Jin** <sup>1,2,\*</sup>, **Gaolong Zhu** <sup>1,2,\*</sup> and **Jia Guo** <sup>1</sup> <sup>1</sup> Department of Geography, Geography and Ocean College, Minjiang University, Fuzhou 350108, China<sup>2</sup> Technology Innovation Center for Monitoring and Restoration Engineering of Ecological Fragile Zone in Southeast China, Ministry of Natural Resources, Fuzhou 350001, China

\* Correspondence: jinsf@tea.ac.cn (S.J.); zhugaolong@163.com (G.Z.); Tel.: +86-18850102506 (S.J.)

**Abstract:** Farmland is the basis for human survival and development. The phenomenon of cropland abandonment has seriously affected national agricultural production and food security. In this study, remote sensing monitoring of abandoned cropland is carried out based on multisource time series remote sensing data using the Google Earth Engine (GEE) cloud platform. Landsat and Sentinel-2 time series data from 2010–2021 were used to obtain monthly synthetic cloud-free image sets in combination with cropland plot data. The time series farmland probability dataset was generated using the random forest classification method. The LandTrendr algorithm was used to extract and analyse the time series cropland probability dataset. Finally, this study also explored the drivers of change in abandoned cropland in Fujian Province. The results show that (1) the LandTrendr algorithm can effectively extract abandoned farmland and avoid the impact of pseudovariation resulting from non-farmland categories. A total of 87.02% of the abandoned farmland was extracted in 2018; 87.50% of the abandoned farmland was extracted in 2020. (2) The abandoned area in Fujian Province fluctuated after a significant increase in 2012, with the abandoned area exceeding 30 thousand hectares. Since 2017, the abandoned area has decreased to slightly below 30 thousand hectares. (3) The regression results of the factors affecting abandoned cropland in Fujian Province show that the increase in the number of agricultural workers and the improvement in soil organic matter content will significantly reduce the area of abandoned cropland in Fujian Province, while the increase in the rate of urbanization, poor road accessibility, and insufficient irrigation conditions will increase the area of abandoned cropland. The results of this study are useful for conducting surveys of cropland abandonment and obtaining timely and accurate data on cropland abandonment. The results of this study are of great significance for the development of effective measures to stop the abandonment of cropland, and ensure the implementation of food security strategies.



**Citation:** Wu, J.; Jin, S.; Zhu, G.; Guo, J. Monitoring of Cropland Abandonment Based on Long Time Series Remote Sensing Data: A Case Study of Fujian Province, China. *Agronomy* **2023**, *13*, 1585. <https://doi.org/10.3390/agronomy13061585>

Academic Editor: Alberto San Bautista

Received: 2 February 2023

Revised: 3 June 2023

Accepted: 7 June 2023

Published: 12 June 2023



**Copyright:** © 2023 by the authors. Licensee MDPI, Basel, Switzerland. This article is an open access article distributed under the terms and conditions of the Creative Commons Attribution (CC BY) license (<https://creativecommons.org/licenses/by/4.0/>).

## 1. Introduction

Agriculture is the industrial basis of national economic construction and development. Farmland resources are the foundation of agricultural development and are fundamental to ensure the quality and safety of agricultural products [1]. However, taking China as an example, China's farmland area was 0.135 billion hectares in 2019, and the per capita farmland area was approximately 0.10 hectare [2–4]. The Chinese government has introduced a series of strict policies and measures to protect farmland, but there is still a tendency for farmland to become “non-food” areas in some regions; this is particularly evident in the phenomenon of cropland abandonment [3].

The abandonment of farmland can cause serious waste of farmland resources, which in turn affects food production [1]. The phenomenon of cropland abandonment in China first

appeared in the mid to late 1980s [2,3]. There are two main factors of cropland abandonment. The first aspect is socioeconomic. On the one hand, the accelerated pace of urbanization has led to the precipitation of rural labour. On the other hand, the migration of the rural population to cities and the aging of the rural population have led to the abandonment of farmland [4]. The second aspect is the agricultural production conditions, which lead farmers to abandon farming due to the inconvenience of farming and low crop yields. It has been shown that regions with predominantly mountainous terrain are more prone to abandonment than regions with plain terrain, under relatively uniform socioeconomic conditions [5,6].

For a long time, the surveying of abandoned farmland was mostly based on survey reporting and field sampling [7,8]. This method is not only time-consuming and labourious, but also inevitably brings errors in information transfer, resulting in inconvenient information updates and poor timeliness [9]. With the continuous development of agricultural remote sensing technology, remote sensing has been gradually applied to crop monitoring [10], yield estimation [11], and disaster early warning [12], which has greatly improved the convenience and timeliness of monitoring agricultural information [13,14]. In particular, the emergence of high-resolution remote sensing images in recent years has substantially enhanced our ability to monitor agricultural information. Remote sensing can quickly obtain information on the spatial distribution of crops, and has the characteristics of a wide identification range and large information content [15]. Compared with traditional methods, this method greatly reduces labour costs. In addition, remote sensing data are convenient for statistics and analysis, and the data format is conducive to building a library for storage. With the emergence of new-generation information technology such as cloud computing and big data, the cloud platform for remote sensing data processing has emerged; it effectively solves the problem of inconvenient storage and the calculation of remote sensing data on personal computers [16]. Modern information technology such as satellite remote sensing and cloud platforms are combined to carry out surveys of abandoned farmland. This approach is of great practical significance for realizing the dynamic monitoring and evaluation of abandoned farmland, and for implementing information-based and refined management.

Fujian Province is located in the hilly region of southeast China, with a unique topography and landscape. The per capita farmland is less than half an acre, and the proportion of ridge fields is large, so the farmland resources are very limited. In addition, some mountainous and hilly areas have poor farming conditions, so the phenomenon of cropland abandonment is particularly prominent. Due to the complex topography, fragmentation of farmland and cloudy and rainy climate in Fujian Province, the application of remote sensing technology in the extraction of abandoned farmland has become very difficult. To this end, this study uses Landsat and Sentinel-2 as the main data sources, based on the Engine cloud platform (GEE) platform. Remote sensing extraction of abandoned farmland in Fujian Province was carried out between 2011 and 2020 to study changes in its characteristics, and to analyse the driving factors of abandonment.

The framework of this thesis is as follows. The first part concerns the extraction of abandoned farmland in Fujian Province. Based on Landsat and Sentinel-2 images as data, the farmland plot data in the land use database are restricted, and the mean value of image elements within the plot boundary is synthesized. Multidimensional classification features were constructed, and the farmland probabilities were output using the random forest algorithm to obtain a time series farmland probability dataset for 2010–2021 in the study area. With 2010 and 2021 as the starting and ending endpoints, segmentation was performed using the LandTrendr algorithm, and the plots with a significant decrease in the probability of farmland from 2011 to 2020 were extracted as abandoned farmland. The second part of this paper concerns the analysis of the extraction results of abandoned farmland in Fujian Province. The third part is the analysis of the influencing factors of abandoned farmland in Fujian Province. The natural and socioeconomic factors related to abandoned farmland were selected, and the abandoned farmland area in each year was

used as panel data to carry out the analysis of the impact factors of abandoned farmland using a multiple regression model.

## 2. Materials and Methods

### 2.1. Definition of Abandoned Land

After completing the research on the actual abandonment situation in the study area and investigating the local farming system, this study chose to define farmland not cultivated for one year or more as abandoned farmland, i.e., abandonment in a narrow sense (Figure 1) [17].



**Figure 1.** Field survey photos of abandoned farmland in 2017 in Puchen County.

### 2.2. Study Area

The geographical location and administrative division of Fujian Province are shown in Figure 2. Fujian Province is located on the southeast coast of China, between  $23^{\circ}33' N \sim 28^{\circ}20' N$  and  $115^{\circ}50' E \sim 120^{\circ}44' E$ . It is 480 kilometres wide from east to west, and 530 kilometres long from north to south, with a land area of 124,000 square kilometres. Fujian has a subtropical maritime monsoon climate. The topography of Fujian Province is complex and diverse, and the influence of nonzonal factors, such as topography and geomorphology, regional differences in water and heat conditions, and vertical divergence, is more obvious therein, resulting in a variety of local microclimates. These conditions provide superior natural conditions of water and heat for the development of farmland and its development and utilization.

The total land area of Fujian Province is approximately 12,396,800 hectares. Among them, farmland covers 1,336,500 hectares, accounting for 10.78% of the total land area. There are three main types of farmland in Fujian Province: paddy fields, watered land and dry land, whose areas are approximately 1,109,400 hectares, 42,500 hectares and 186,000 hectares, respectively, accounting for 82.92%, 3.18% and 13.90% of the total farmland area, respectively.

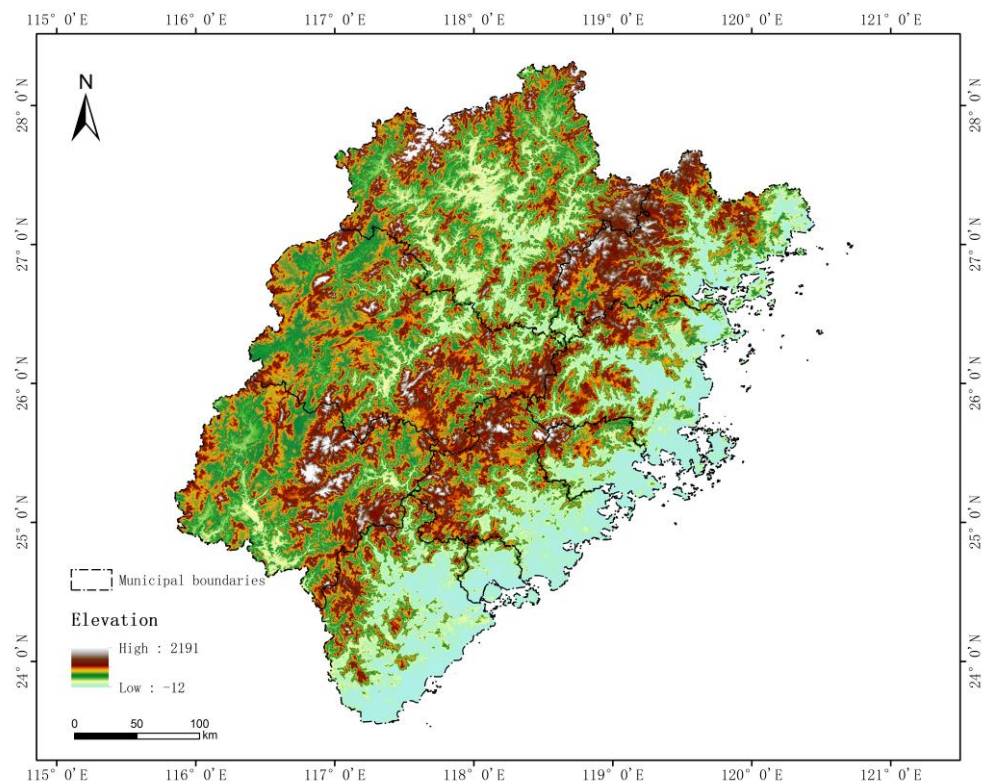


**Figure 2.** Location of the study area.

### 2.3. Research Data

#### 2.3.1. Remote Sensing Data

The remote sensing data used in this study were obtained from the Google Earth Engine cloud platform (GEE). GEE is a cloud-based geospatial information visualization and analysis platform jointly developed by Google, Carnegie Mellon University, and the United States Geological Survey (USGS) [18]. GEE relies on Google's own cloud platform, Google Cloud Platform (GCP), to provide users with petabytes of data-computing power [16]. The GEE platform has been widely used for land use [19,20], urban sprawl [21,22], vegetation information extraction [23,24], and climate-related changes [25,26]. For example, Zeng et al. [27] used GEE to map farmland in Southeast Asia, Burke and Lobell [28] estimated the yield of tens of thousands of smallholder farms in Africa, and Tuckett et al. [29] used high-resolution satellite-derived ice velocity data to analyse the effect of atmospheric warming on the rate of glacier melting.

The satellite images used in this study are Landsat and Sentinel-2 data from the GEE platform database, which includes top of atmosphere (TOA) and surface reflectance (SR) data. In this study, radiometrically corrected Landsat SR data are used. Two processing levels of Sentinel-2 data are available in the GEE database: the L2A level and L1C level. In the GEE platform database, the datasets of L2A and L1C were named COPERNICUS/S2\_SR and COPERNICUS/S2, respectively. L2A contains the atmospherically corrected atmospheric bottom reflectance data, and L1C contains the orthorectified and geometrically refined atmospheric apparent reflectance product.

Using the GEE platform, Landsat and Sentinel-2 data have been processed through radiometric calibration, atmospheric correction and geometric correction, which has reduced the influence of external conditions such as atmosphere, illumination and terrain and geometric distortion. However, because the study area has a subtropical monsoon climate, it is cloudy and rainy all year round, so the effective optical image is insufficient; this may easily cause discontinuity and the loss of time series data, so cloud removal processing is required. Here, the cloud mask method is used to remove the cloud from the data. The cloud mask method uses the CFMASK (the C function of mask) algorithm in GEE

to generate a QA band for image data to represent the attribute of pixel quality. The third and fourth digits of the QA band of Landsat5 and Landsat7 image data represent cirrus and cloud information. The second and third digits of the QA band of Landsat8 image data represent cirrus and cloud information. The tenth and eleventh bits of the Sentinel-2 image data represent cirrus and cloud information, and a value of 0 means that there is no cloud or cirrus in this pixel; a value of 1 means that there is a cloud or cirrus. The Landsat and Sentinel-2 data were screened through the QA band for cirrus and cloud information, respectively, and the cloud-containing pixels were set as null values to generate a mask; the mask function was used to mask the data set, and then a loop was constructed.

### 2.3.2. Basic Geographic Data

The basic geographic data are mainly from the 2018 farmland quality database of Fujian Province and the database of the Third National Land Survey of Fuzhou City. The farmland quality database contains information on the farmland patches, farmland quality class, road accessibility, topographic slope and irrigation guarantee rate in Fujian Province. The database also contains land use types other than farmland. The database also contains information on the cultivation status of farmland, which is used to correct the classification sample data.

### 2.3.3. Statistical Data

Statistical data were obtained from the Fujian Provincial Statistical Yearbook and the statistical yearbooks of each prefecture-level city. The crop cultivation area, food and non-food crop cultivation, natural population growth rate, urban population data, and per capita disposable income of rural residents and agricultural employees data were obtained at the municipal level from 2011 to 2020.

### 2.3.4. Validation Sample Data

The farmland validation samples are the field sampling data. There were 6373 farmland sample points in 2017, and 7000 farmland sample points in 2018. The abandoned farmland validation samples are 262 abandoned farmland sample points in 2018 and 296 abandoned farmland sample points in 2020. The distribution of farmland and abandoned farmland validation sample points is shown in Figure 3.

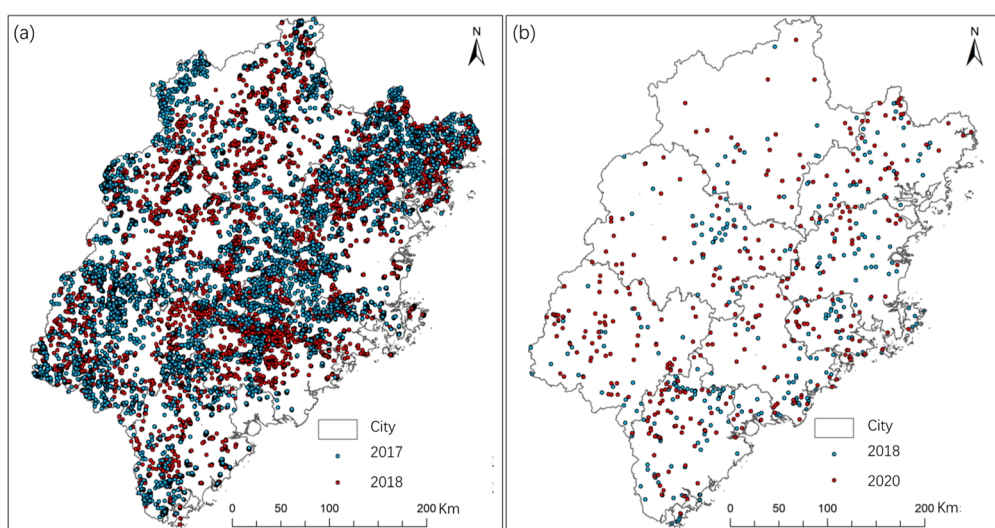


**Figure 3.** Validation sample point distribution map, (a): validation point of the farmland in 2017 and 2018; (b) validation point of the abandoned farmland in 2018 and 2020.

## 2.4. Abandoned Farmland Extraction Method

### 2.4.1. Construction of Abandoned Farmland Based on Farmland Boundaries

Existing studies on the extraction of abandoned farmland are mostly pixel-based, and all the geographical elements in the study area are identified and interpreted; thus, they are susceptible to the “pepper effect” caused by mixed image elements. In addition, the farmland in this study area is mostly distributed in hilly and mountainous areas, with fragmented plots, complex shapes and sporadic distribution, all of which are more likely to cause errors. As a basic plot unit, farmland has obvious boundaries and single ownership, so using farmland boundaries to control farmland information extraction can effectively improve the errors caused by mixed image elements [30,31]. Farmland parcel boundaries are stable and reusable, and gaining approval to change from farmland to another land use type is very difficult in China; thus, only a few areas farmland are converted to other land types every year.

Therefore, this study uses the farmland plots in the farmland quality database to limit the extent of farmland. By synthesizing the data of each waveband of the 12 monthly averages for each year, the image elements in the plot extent are averaged. In turn, a dataset containing the mean synthesis data of farmland plots in each waveband for 12 periods of each year is obtained. By calculating the mean synthesis in the plot range, the pepper noise effect of the mixed image elements at the edge of the farmland can be reduced.

### 2.4.2. Construction of Multidimensional Classification Feature for Abandoned Farmland

#### 1. Spectral characteristics

The Landsat and Sentinel-2 multiband data information includes Blue, Green, Red, NIR, SWIR1 and SWIR2 in a total of six bands. Therefore, in this study, the maximum, minimum, mean and median values of each image element of the farmland block in each band were calculated as the original spectral features that would make up the farmland classification features.

Vegetation indices are various indices obtained by combining visible and near-infrared bands of remote sensing images according to the spectral characteristics of vegetation, which can effectively reflect the characteristics of surface vegetation. There are approximately 40 vegetation indices available [32], which are widely used in land cover, vegetation classification, crop yield estimation and environmental monitoring. Among them, the normalized difference vegetation index (NDVI), enhanced vegetation index (EVI), soil-adjusted vegetation index (SAVI), and improved soil-adjusted vegetation index (MSAVI) are widely used in land cover, vegetation classification, crop yield estimation, and environmental monitoring. The SAVI and modified soil-adjusted vegetation index (MSAVI) are more commonly used [33].

The NDVI index is one of the most commonly used vegetation indices in abandoned farmland extraction. This index enhances the contrast of reflectance in the NIR and red bands through non-linear stretching, which can effectively detect vegetation growth status and vegetation cover and eliminate some radiometric errors. However, the sensitivity in the high vegetation cover region is low. The NDVI index contains defects such as atmospheric noise. To overcome this drawback, the EVI adds a blue band to enhance the vegetation signal and correct the effect of soil background and aerosol scattering. Compared with the NDVI index, the SAVI index adds a soil conditioning factor L, which is determined according to actual conditions to reduce the effect of the soil background. However, it is only applicable under ideal conditions. For this reason, the MSAVI index was proposed. The influence of the soil background on vegetation detection is directly attenuated by quantification. It improves the shortcomings of the SAVI index and enhances vegetation detection, which is more suitable for studies of vegetation cover information extraction. Combining the advantages and disadvantages of the above indices, NDVI, EVI and MSAVI indices were selected as classification features in this study, and the maximum, minimum, mean and median values were calculated. These statistics can reflect the physical

characteristics of farmland to a certain extent, and improve the quality of classification results. The formulas for calculating each index are shown below.

$$\text{NDVI} = \frac{\rho_{\text{NIR}} - \rho_{\text{Red}}}{\rho_{\text{NIR}} + \rho_{\text{Red}}} \quad (1)$$

$$\text{EVI} = 2.5 \times \left( \frac{\rho_{\text{NIR}} - \rho_{\text{Red}}}{\rho_{\text{NIR}} + 6.0 \times \rho_{\text{Red}} - 7.5 \times \rho_{\text{Blue}} + 1} \right) \quad (2)$$

$$\text{MSAVI} = \frac{2 \times \rho_{\text{NIR}} + 1 - \sqrt{(2 \times \rho_{\text{NIR}} + 1)^2 + 8 \times (\rho_{\text{NIR}} - \rho_{\text{Red}})}}{2} \quad (3)$$

where  $\rho_{\text{NIR}}$ ,  $\rho_{\text{Red}}$ , and  $\rho_{\text{Blue}}$  are spectral features of the bond of NIR, Red, and Blue, respectively. Since the growth of crops is disturbed by human factors, the crops' physical characteristics are significantly different from those of natural vegetation. In particular, most crops demonstrate harvesting phenomena that produce sudden changes in the ground reflectance curve. Therefore, this study captures the phenological changes of crops to a large extent by using the time series remote sensing spectral features of one period per month for 12 periods throughout the year. In turn, we can distinguish farmland with cultivation in the current year from abandoned land with grass or tree growth.

## 2. Texture characteristics

Texture is a pattern that reflects two-dimensional changes in grayscale and colour on the surface of an object; it is a representation of the content of grayscale changes on the surface of an object. The cultivation process of farmland produces distinctive texture features that make it very different from other land types. It is one of the main features of the classification of farmland.

The currently available texture feature extraction methods are mainly divided into four categories: statistical methods, model methods, signal-processing methods and structural methods [34]. Among them, statistical methods are based on the grayscale properties of image elements and adjacent image elements. The study of the first-order, second-order or higher-order statistical properties of the grayscale in the image element and its pro-domain is simple and easy to implement. In particular, the grey level cooccurrence matrix (GLCM) method [35] is recognized as an effective method with strong adaptability and robustness [36]. Starting from a pixel point with grey level  $i$ , the grey level value at a point leaving a fixed location (separated by a distance  $d$  and orientation  $\theta$ ) is found using the 14 statistics proposed by Haralick et al. [37]; these are calculated based on the GLCM: namely, energy (Asm), entropy (Ent), contrast (Contrast), uniformity (Idm), correlation (Corr), variance (Var), and mean (Savg), sum variance (Svar), sum entropy (Sent), difference variance (Dvar), difference entropy (Dent), correlation information measures (Imcorr1, Imcorr2), and the maximum correlation coefficient (MaxCorr) [37]. In addition, the GEE contains the four statistics of difference (Diss), inertia (Inertia), cluster shading (Shade) and cluster prominence (Prom), as proposed by Connors et al. [38], for a total of 18 statistics. The texture characteristics of farmland are closely related to the changes in vegetation, and to avoid redundancy of data, NDVI images calculated from cloud-free annual mean synthetic images were chosen for this study.

## 3. Terrain characteristics

Due to the large area of hilly areas in Fujian Province, farmland is usually distributed in areas with relatively flat terrain and low elevation. Therefore, the topographic features of hilly mountainous areas are also one of the main features to be considered for extracting farmland information. Within the GEE platform, 30 m resolution SRTMGL1\_003 data are used to calculate two feature components, elevation and slope, which are involved in the construction of the classification feature set. This study also utilized the SRTM (Shuttle Radar Topography Mission) digital elevation model and land use classification products

from the PIE Remote Sensing Cloud Service Platform (<https://engine.piesat.cn/>, accessed on 1 February 2023).

### 2.5. Data Processing

#### 2.5.1. Random Forest Classification Method

Random forest (RF) [39] is an algorithm that integrates multiple decision trees through the idea of integration learning. RF has a good accuracy rate and can efficiently perform operations on large datasets. With the ability to handle input samples with multidimensional classification features and without dimensionality reduction, it is currently the most commonly used and excellent classification algorithm [40]. Random forests have been widely used in the fields of land use classification, artificial intelligence and data mining [41,42].

#### 2.5.2. Extraction of Abandoned Farmland Based on the LandTrendr Algorithm

The LandTrendr (Landsat-based detection of Trends in Disturbance and Recovery) algorithm is a method proposed by Kenedy et al. [43] in 2010 to extract spectral trajectories of surface change from annual Landsat time series overlays (LTS). The method combines two themes of time series analysis: capturing short-term events and smoothing long-term trends [44]. The results of the time series farmland probabilistic classification images from 2010 to 2021 were exported to the resource manager of the GEE platform, after masking with farmland plots, and merged into image sets. In this study, the farmland probability mutation points for 2011–2020 were extracted based on the parameters required for the LandTrendr algorithm, using 2010 and 2021 as the start and end points, respectively. Finally, a typical abandoned farmland time series probability curve and a non-abandoned farmland time series probability curve were generated.

### 2.6. Model Evaluation

The model evaluation in this study uses the overall accuracy (OA), Kappa coefficient, user accuracy (UA), and producer accuracy (PA), calculated based on a confusion matrix. The specific formulas are shown in Table 1.

**Table 1.** Quantitative evaluation index calculation formula.

Indices	Formulas	Descriptions
Overall accuracy (OA)	$OA = \frac{X_{ii}+X_{jj}}{N}$	Ratio of the number of correctly classified category pixels to the total number of category pixels [41].
Kappa coefficient	$Kappa = \frac{X_{ii}+X_{jj}-q}{N-q}$ $q = \frac{(X_{ii}+X_{jj})(X_{ii}+X_{ji})+(X_{jj}+X_{ij})(X_{jj}+X_{ji})}{N}$	For evaluating the consistency of classification results [41].
User accuracy (UA)	$UA = \frac{X_{ii}}{X_{ii}+X_{ji}}$	Ratio of the number of correctly classified pixels in a category to the total number of pixels in that category [42].
Producer's accuracy (PA)	$PA = \frac{X_{ii}}{X_{ii}+X_{ij}}$	Ratio of the number of correctly classified pixels of a category to the total number of true reference pixels of that category [41].

$X_{ii}$  is the number of samples correctly classified as farmland category,  $X_{ij}$  is the number of samples not correctly classified as farmland category,  $X_{jj}$  is the number of samples correctly classified as nonfarmland category,  $X_{ji}$  is the number of samples not correctly classified as non-farmland category, and  $N$  is the total number of samples.

### 2.7. Calculation of Cropland Abandonment Rate

The ratio of the abandoned land area to the overall farmland area per year was set as the abandonment rate of farmland in this study, using the following formula:

$$P_y = \frac{A_j}{A_i} \times 100\% \quad (4)$$

where  $P_y$  is the abandonment rate in year  $y$ ;  $A_j$  is the abandoned area in year  $i$ ; and  $A_i$  is the overall arable area.

### 2.8. Driving Factors for Abandoned Farmland

In this study, the factors that may influence the area of abandonment in each prefecture-level city in Fujian Province were selected from both socioeconomic factors and natural condition factors [45–47]. The selected influencing factors affecting abandonment are shown in Table 2.

**Table 2.** Description of cropland abandonment variables.

Name of Variables	Description of Variables
Natural population growth rate	Trends and rates of natural population growth (%).
Agricultural practitioners	Number of people engaged in agricultural labour (people).
Urbanization rate	Urban population/total population (%).
Per capita disposable income of rural residents	Per capita disposable income of rural residents (yuan).
Soil organic matter content	Organic matter content within unit land (g/kg).
Field road accessibility	Distance between farmland and roads with a road width of 3 m or more (meters).
Irrigation guarantee rate	The irrigation condition of the farmland is 1–4 levels from high to low, with level 1 being fully satisfied, level 2 being basically satisfied, level 3 being generally satisfied, and level 4 is no irrigation condition.

## 3. Results

### 3.1. Classification Feature Filtering

In this study, there are 36 spectral features, 18 texture features and 2 topographic features that respond to the physical characteristics of the features, totaling 56 features. Table 3 shows that among the spectral features, MSAVI index minimum (MSAVI\_minum), MSAVI index median (MSAVI\_median), NDVI index minimum (NDVI\_minum), NDVI index median (NDVI\_median) and red\_median have high importance and high differentiability in land use classification.

**Table 3.** Importance of spectral characteristics.

Serial Number	Features	Importance	Serial Number	Features	Importance
1	EVI_max	145.46	19	SWIR2_median	154.61
2	EVI_mean	145.37	20	SWIR2_minum	159.91
3	EVI_median	158.34	21	blue_max	120.54
4	EVI_minum	152.71	22	blue_mean	117.31
5	MSAVI_max	163.26	23	blue_median	150.53
6	MSAVI_mean	178.35	24	blue_minum	119.13
7	MSAVI_median	185.75	25	green_max	144.21
8	MSAVI_minum	188.52	26	green_mean	145.22
9	NDVI_max	118.92	27	green_median	144.94
10	NDVI_mean	161.42	28	green_minum	120.27
11	NDVI_median	167.50	29	nir_max	122.98
12	NDVI_minum	175.91	30	nir_mean	152.55
13	SWIR1_max	148.54	31	nir_median	152.08
14	SWIR1_mean	117.82	32	nir_minum	160.02
15	SWIR1_median	117.06	33	red_max	123.66
16	SWIR1_minum	144.78	34	red_mean	115.32
17	SWIR2_max	151.14	35	red_median	181.58
18	SWIR2_mean	155.65	36	red_minum	145.12

From Table 4, it can be seen that among the texture features, sum average (Savg) and cluster shading (Shade) have high importance and are highly distinguishable in the land use classification.

**Table 4.** Importance of texture features.

Serial Number	Features	Importance	Serial Number	Features	Importance
1	Asm	74.11	10	Imcorr2	80.37
2	Contrast	97.56	11	Inertia	94.87
3	Corr	97.81	12	MaxCorr	0.00
4	Dent	60.58	13	Prom	100.96
5	Diss	85.77	14	Savg	145.60
6	Dvar	83.89	15	Sent	74.65
7	Ent	60.60	16	Shade	146.69
8	Idm	91.83	17	Svar	92.68
9	Imcorr1	84.24	18	Var	86.92

As shown in Table 5, the statistics of topographic features have high importance in the land use classification of Fujian Province, especially the importance of elevation features, which is much higher than that of other features.

**Table 5.** Importance of terrain features.

Serial Number	Features	Importance
1	Slope	185.86
2	Elevation	264.01

By ranking the feature importance, it was found that a significant sudden drop in feature importance occurred at 144, so features with importance above 144 were selected, and redundant features with lower importance were removed. After screening, the study selected 30 features for classification, and these classification features are shown in Table 6.

**Table 6.** Importance of classification characteristics.

Serial Number	Features	Importance	Serial Number	Features	Importance
1	elevation	264.01	16	EVI_minumum	152.71
2	MSAVI_minumum	188.52	17	nir_mean	152.55
3	SLOPE	185.86	18	nir_median	152.08
4	MSAVI_median	185.75	19	SWIR2_max	151.14
5	red_median	181.58	20	blue_median	150.53
6	MSAVI_mean	178.35	21	SWIR1_max	148.54
7	NDVI_minumum	175.91	22	shade	146.69
8	NDVI_median	167.50	23	savg	145.60
9	MSAVI_max	163.26	24	EVI_max	145.46
10	NDVI_mean	161.42	25	EVI_mean	145.37
11	nir_minumum	160.02	26	green_mean	145.22
12	SWIR2_minumum	159.91	27	red_minumum	145.12
13	EVI_median	158.34	28	green_median	144.94
14	SWIR2_mean	155.65	29	SWIR1_minumum	144.78
15	SWIR2_median	154.61	30	green_max	144.21

### 3.2. Time Series Farmland Probability Classification

Figure 4 shows the results of the time series farmland probability classification from 2010 to 2021.

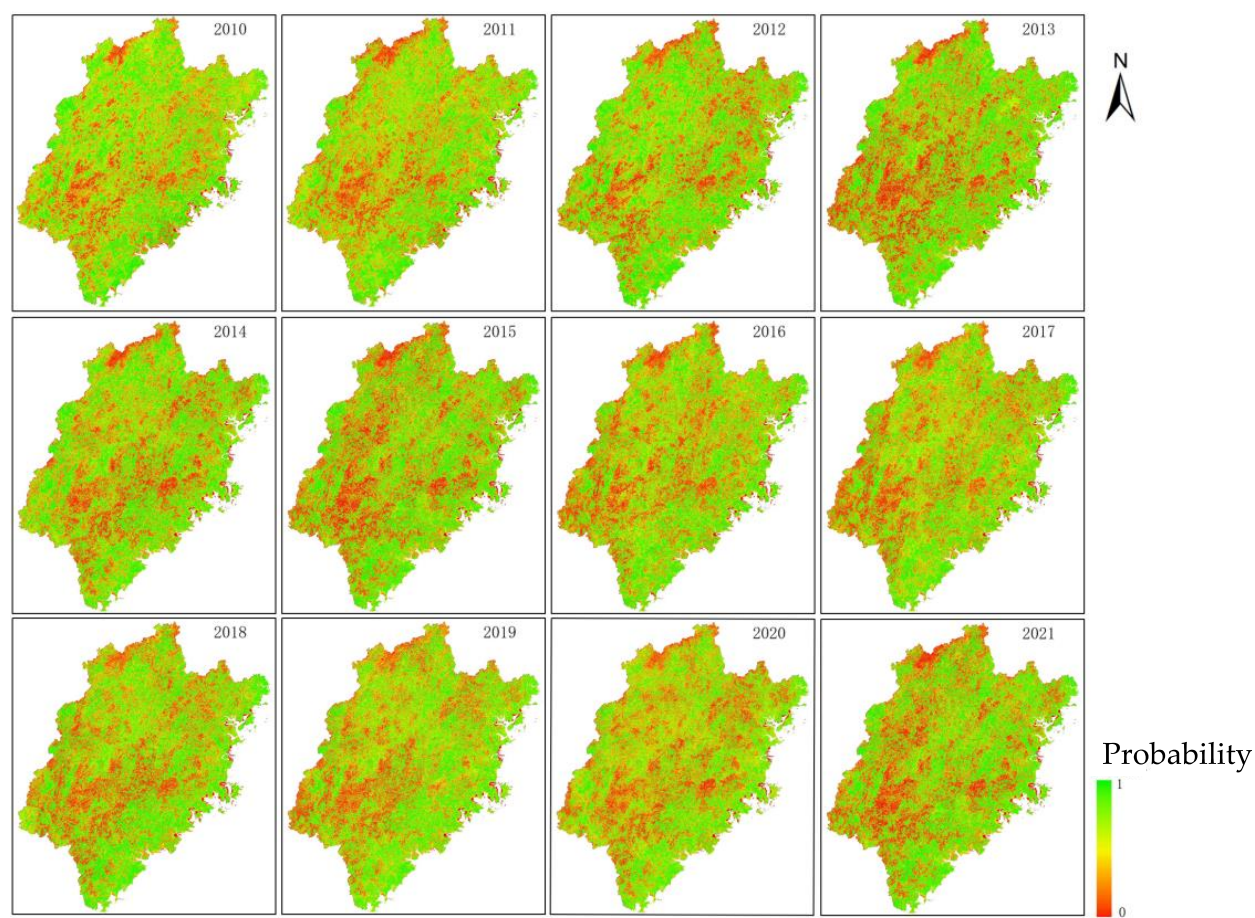


**Figure 4.** Farmland probability classification results in Fujian Province, China.

The results of the quantitative evaluation using the 10-fold cross-validation (10-fold cross-validation) method are shown in Table 7. The results show that the average overall precision for each year from 2010 to 2021 is 0.94, the average user precision is 0.96, the average producer precision is 0.96, and the average Kappa coefficient is 0.85, indicating that the classification quality is excellent.

**Table 7.** Accuracy evaluation index statistics.

Years	PA	UA	OA	Kappa
2010	0.95	0.94	0.94	0.87
2011	0.96	0.94	0.95	0.89
2012	0.93	0.95	0.93	0.86
2013	0.96	0.96	0.93	0.79
2014	0.96	0.94	0.95	0.89
2015	0.94	0.96	0.95	0.88
2016	0.95	0.97	0.95	0.89
2017	0.95	0.97	0.94	0.84
2018	0.97	0.97	0.96	0.85
2019	0.96	0.96	0.93	0.79
2020	0.96	0.97	0.95	0.84
2021	0.98	0.97	0.96	0.88

### 3.3. The Results of LandTrendr Extraction

The time series probability curves of typical abandoned farmland and the time series probability curves of nonabandoned farmland generated from the LandTrendr fitting results are shown in Figure 5.

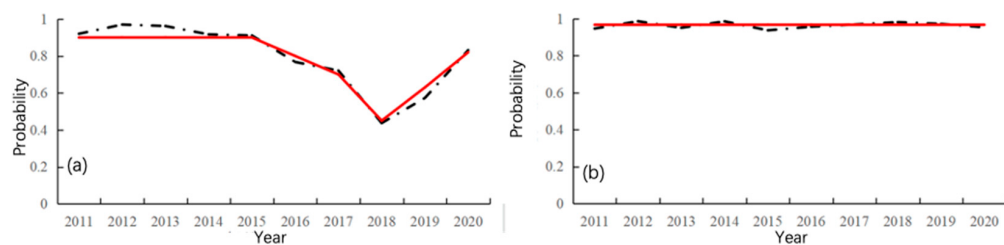


**Figure 5.** LandTrendr fitting results. (a) Typical abandoned farmland; (b) Non-abandoned farmland. The black dotted line represents the probability of farmland, and the red line represents the fitted lines found using LandTrendr.

### 3.4. Model Validation

The validation results are shown in Table 8. A total of 6360 sample points of farmland in 2017 were verified as correct, 13 were misclassified as abandoned farmland, and the validation accuracy was 99.80%; 6981 sample points in 2018 were verified as correct, 19 were misclassified as abandoned farmland, and the validation accuracy was 99.73%. A total of 231 sample points of abandoned farmland in 2018 were verified as correct, and the validation accuracy was 87.02%. In 2020, 259 abandoned farmlands were verified as correct, with a verification accuracy of 87.50%. The results of the verification of the partial abandonment of farmland are shown in Figure 6, with the image of farmland on the left (Figure 6a,b) and the image of abandoned farmland on the right (Figure 6c,d). These images are the verified fields for validation.

**Table 8.** The results of the accuracy verification.

Years	Validation Accuracy of Farmland	Validation Accuracy of Abandoned Farmland
2017	99.80%	-
2018	99.73%	87.02%
2020	-	87.50%



**Figure 6.** Partially abandoned farmland accuracy verification. (a,b) is the validation farmland image; (c,d) is the validation abandoned farmland image; the area surrounded by the red lines is the abandoned farmland.

### 3.5. Analysis of the Change in Abandoned Farmland Area in Fujian Province

Overall, as shown in Table 9, the maximum area of abandoned farmland in Fujian Province from 2011 to 2020 was 36.94 thousand hectares, the minimum area was 23.12 thousand hectares, and the average abandoned area was 31.35 thousand hectares. The overall trend of abandoned farmland area fluctuated, without a significant increasing or decreasing trend. Among them, the area of abandoned farmland slightly decreased from 2018 to 2020, probably due to the promotion of land transfer and farmland quality protection and improvement projects after 2018. The total area of abandoned farmland has decreased to below 30 thousand hectares.

**Table 9.** Area of abandoned farmland by prefecture-level cities in Fujian Province from 2011 to 2020. (Unit: Thousands of hectares).

Prefecture-Level Cities	2011	2012	2013	2014	2015	2016	2017	2018	2019	2020
Fuzhou	1.74	4.48	2.47	3.11	2.97	3.17	2.88	3.33	1.87	2.92
Ningde	1.66	5.09	1.75	3.72	3.46	3.01	4.01	3.56	2.65	3.92
Putian	1.05	2.14	1.68	2.33	2.37	1.90	1.80	1.77	1.09	1.67
Quanzhou	2.79	3.30	3.28	3.40	3.84	3.85	3.32	3.14	2.55	3.22
Sanming	3.32	3.16	4.10	3.60	3.85	4.75	4.63	3.98	4.40	3.84
Xiamen	0.21	0.29	0.21	0.21	0.30	0.30	0.30	0.25	0.29	0.46
Zhangzhou	3.09	6.80	5.83	8.04	7.71	4.00	3.94	4.81	4.44	5.31
Longyan	7.59	8.56	9.74	5.10	9.24	9.12	10.54	6.24	7.22	5.04
Nanping	1.66	2.16	1.99	2.33	3.20	3.70	2.86	2.45	2.89	3.21
The whole province	23.12	35.97	31.04	31.83	36.94	33.79	34.27	29.54	27.40	29.59

As shown in Table 10, the abandoned farmland area in Fujian Province accounts for less than 2.50% of the total farmland area; the maximum abandonment rate is 2.32%, the minimum abandonment rate is 1.45%, the average abandonment rate is 1.97%, and the overall trend is the same as that of the abandoned farmland area. The largest area in Fujian Province is Longyan City, 2011–2020, with a maximum abandonment rate of 5.51%, a minimum abandonment rate of 3.01%, and an average abandonment rate of 4.67%, all of which are higher than those in other regions. The cropland abandonment rate in Zhangzhou was second to that in Longyan city, and in 2012–2015, the abandonment rate was greater than 3%. The minimum abandonment rate in Fujian Province occurred in Nanping City, 2011–2020, with a maximum abandonment rate of 1.55%, a minimum abandonment rate of 0.70%, and an average abandonment rate of 1.11%. Except for Longyan City and Zhangzhou City, the abandonment rate of all regions in Fujian Province is less than 3.50%, and the trend of change is small.

### 3.6. Driving Factors of Cropland Abandonment

To find out the roles of driving factors effecting farmland abandonment, a multiple linear regression method was performed. Among the factors influencing abandoned farmland in Fujian Province, agricultural workers and soil organic matter content had a negative effect on abandoned farmland area, indicating that an increase in agricultural workers and soil organic matter content would reduce the area of abandoned farmland. The urbanization rate, field road accessibility and irrigation guarantee rate had a positive effect on the area of abandoned farmland, indicating that an increase in the urbanization rate, poor road accessibility and insufficient irrigation conditions would increase the area of abandoned farmland (Table 11). In detail, the regression coefficient of agricultural workers on the area of abandoned farmland in Fujian Province is  $-0.334$ , which indicates that every 1% increase in agricultural workers will reduce the area of abandoned farmland by 0.334%. The regression coefficient of the urbanization rate on the area of farmland abandoned in Fujian Province is  $0.475$ , which indicates that for every 1% increase in the urbanization

rate, the area of abandoned land will increase by 0.475%. The regression coefficient of soil organic matter content on the area of farmland abandoned in Fujian Province is  $-0.172$ . This indicates that every 1% increase in soil organic matter content will reduce the area of abandoned land by 0.172%. The regression coefficient of the accessibility of field roads on the abandoned area of farmland in Fujian Province was 0.032, which indicated that every 1% increase in the accessibility of field roads would increase the abandoned area by 0.032%. The regression coefficient of the irrigation guarantee rate is 1.104, which indicates that every 1% increase in irrigation guarantee rate registration will reduce the abandoned area by 1.104%.

**Table 10.** Fujian Province prefecture-level cities' 2011–2020 abandonment rates (Unit: %).

Prefecture-Level Cities	2011	2012	2013	2014	2015	2016	2017	2018	2019	2020
Fuzhou	1.12	2.87	1.58	2.00	1.91	2.03	1.85	2.14	1.20	1.87
Ningde	1.02	3.12	1.07	2.28	2.12	1.85	2.46	2.18	1.63	2.41
Putian	1.43	2.91	2.29	3.17	3.23	2.59	2.45	2.41	1.48	2.27
Quanzhou	1.92	2.27	2.26	2.34	2.64	2.65	2.29	2.16	1.76	2.22
Sanming	1.69	1.61	2.09	1.83	1.96	2.42	2.36	2.03	2.24	1.95
Xiamen	1.11	1.54	1.11	1.11	1.59	1.59	1.59	1.32	1.54	2.44
Zhangzhou	1.73	3.80	3.26	4.49	4.31	2.24	2.20	2.69	2.48	2.97
Longyan	4.53	5.11	5.81	3.04	5.51	5.44	6.29	3.72	4.31	3.01
Nanping	0.70	0.91	0.83	0.98	1.34	1.55	1.20	1.03	1.21	1.35
The whole province	1.45	2.26	1.95	1.99	2.32	2.12	2.15	1.85	1.72	1.85

**Table 11.** Fujian Province prefecture-level cities' 2011–2020 abandonment rates (Unit: %).

Variables	Regression Coefficient (STD)
Natural population growth rate	0.960 (1.00)
Agricultural practitioners	$-0.344^{***}$ (7.34)
Urbanization rate	0.475 ** (2.81)
Per capita disposable income of rural residents	0.299 (1.59)
Soil organic matter content	$-0.172^{***}$ (6.25)
Field road accessibility	0.032 * (2.60)
Irrigation guarantee rate	1.104 *** (9.25)
Constant term	$-6.959^{***}$ ( $-3.46$ )
Sample size	90
R <sup>2</sup>	0.900

\* , \*\* , \*\*\* denote  $p < 0.1$ ,  $p < 0.05$  and  $p < 0.01$ , respectively.

## 4. Discussion

### 4.1. Extraction of Abandoned Farmland Based on Remote Sensing Index Time Series Change Detection

Time series change detection based on remote sensing indices provides a means to extract information on abandoned farmland with higher temporal resolution, and can sensitively detect changes in farmland utilization. Among them, the normalized difference vegetation index (nDVI) is the main remote sensing index for detecting temporal changes in cropland abandonment; it has high recognition efficiency and accuracy in crop spectra and phenological characteristics. According to the narrow definition of abandoned land, abandoned land is land that has been abandoned for a long period of time due to natural or human causes, and has lost the life cycle of crop “sowing, growing and harvesting”. Therefore, the NDVI time series shows a reduced peak, and some scholars use this feature to identify fallow farmland and distinguish between fallow and rotational fallow land [1,48]. The results showed that the NDVI difference threshold interval of abandoned land was determined using the proportion of abandoned farmland in different zones, and the accuracy of this classification method in extracting abandoned farmland was 92% [49]. In addition, the development of computer technology has led an increasing number of scholars to expand the detection object from image elements to plots using object-oriented, edge detection and multiscale segmentation methods [50,51]. As the most basic individual unit of farmland, the plot has obvious boundaries, a single crop, and obvious characteristics. Therefore, using farmland plots as the detection unit can effectively reduce errors and compensate for the lack of available remote sensing images in some areas by using image segmentation techniques [52].

In this study, the LandTrendr algorithm was used to extract the distribution of abandoned farmland from 2011 to 2020. The results showed that the validation accuracy of the sample points of farmland in 2017 was 99.80%; the validation accuracy in 2018 was 99.73%. The validation accuracy of the sample points of abandoned farmland in 2018 was 87.02%; the validation accuracy of the sample points of abandoned farmland in 2020 was 87.50%. Due to the differences in crop types in different regions, the change in the NDVI index alone in regions with complex cultivation situations cannot fully reflect the process of abandoned farmland. In this study, using the spectral characteristics of integrated remote sensing images, multiple vegetation index characteristics, multitemporal vegetation index change characteristics and terrain feature analysis, the results of the study proved able to better detect abandoned farmland [53–55].

### 4.2. Drivers of Cropland Abandonment

Cropland abandonment is the result of a combination of factors. Within the same region, the risk and extent of cropland abandonment varies among different types of farmland and different types of farmers. The factors influencing cropland abandonment vary from country to country [56]. Prishchepov et al. [57] studied the causes of cropland abandonment in Russia from 1990 to 2000, and found that the main factor of abandonment was labour shortage due to low grain production and low population density [58]. The results of Benayas’ study concluded that the dominant factor of cropland abandonment was socioeconomic development, with farmers moving to towns in search of quality work opportunities in farming, thereby leading to the precipitation of rural labour. Second, natural aspects include the erosion of farmland [58]. Gellrich et al. [59] studied the causes of cropland abandonment in mountainous areas of Switzerland, and the results of their study indicated that the main reasons for abandonment were insufficient effective soil thickness, sloping terrain, and poor road accessibility in mountainous areas [59]. In addition, some countries have abandoned farmland due to war, for example, Iraq, Colombia, and Yugoslavia, where some farmland was abandoned due to the effects of war [60,61].

In this study, the regression analysis showed that as the main labour force for farming, an increase in the number of agricultural workers can effectively solve the problem of an insufficient agricultural labour force and reduce the abandonment of farmland. These

results were consistent with the abandonment of farmland in Russia [58], which implies that people will be one of the main ways to reduce the abandonment of farmland. Further, urbanization is one of the main factors affecting rural labour rates. Urbanization leads to the widening of the gap between urban and rural living standards, and income from non-agricultural industries is much higher than income from farming, resulting in the transfer of young rural labourers to cities [56–59]. In this study, as shown in above, Fujian Province is located in the hilly mountainous area in the southeast, and the main industries are industrial rather than agricultural. Agriculture is already disadvantaged, and coupled with the development of urbanization, there are various job opportunities in high-income non-agricultural industries, leading to a large number of rural labourers abandoning inefficient agriculture and moving to cities. This means that if the urbanization rate continues to increase in the future, more abandoned farmland will appear. Further, we also found that the higher the soil organic matter content is, the better the fertility conditions of the farmland, which is conducive to crop yield, and an increase in yield means higher profitability [59]. Thus, the better the soil conditions of farmland are, the smaller the abandoned area of farmland. In terms of social support, with improvements in people's living standards and the promotion of rural road construction, farmers have gradually abandoned remote farmland that has inconvenient traffic conditions [61]. Therefore, an increase in the accessibility of field roads increases the abandonment rate of farmland. Water resources are essential and important for crop growth; good irrigation conditions are beneficial to crop growth and increase crop yield. In contrast, poor irrigation conditions mean farmers need to collect water for irrigation or build canals to improve irrigation conditions, and this increases the costs of farming. The irrigation guarantee rate directly affects the growth of crops, so the poorer the irrigation condition is, the higher the probability of farmers abandoning farmland.

## 5. Conclusions

In this study, probabilistic information extraction of farmland, identification and distribution characteristics analysis of abandoned farmland, and a study of the impact factors of abandoned farmland were carried out based on the GEE cloud platform, with Fujian Province as the chosen study area. Here, Landsat images and Sentinel-2 images were used as data sources, and a multidimensional classification feature set was combined with farmland plot boundaries after filtering to obtain a time series farmland probability dataset. The average overall accuracy was 0.94, the average Kappa coefficient reached 0.85, the average user accuracy was 0.96, and the average producer accuracy was 0.96, using a random forest classification algorithm. Further, the LandTrendr algorithm showed a high validation precision in extracting the distribution of abandoned farmland from 2011 to 2020. The abandoned area in Fujian Province fluctuated after a significant increase in 2012, and the abandoned area was above 30 thousand hectares. Since 2017, the abandoned area has been reduced to slightly below 30 thousand hectares. Finally, we also showed that an increase in the number of agricultural workers and an increase in soil organic matter content will significantly reduce the area of abandoned land in Fujian Province, while an increase in the urbanization rate, inconvenient road conditions, and insufficient irrigation conditions will aggravate the abandoned land in Fujian Province. Although the boundaries were extensively considered, the farmland may still have changed slightly over the years, which may have caused the boundaries of the farmland to change. In addition, a method of validation for larger-scale spatio-temporal long-term abandoned farmland is still a work in progress. Therefore, more land use databases and more methods of validating extracted abandoned farmland should be considered in the future.

**Author Contributions:** Conceptualization, S.J. and G.Z.; methodology, J.W.; software, J.W. and J.G.; validation, J.W., S.J. and G.Z.; formal analysis, S.J. and J.W.; investigation, J.W., S.J. and G.Z.; resources, G.Z.; data curation, S.J. and G.Z.; writing—original draft preparation, J.W., S.J. and G.Z.; writing—review and editing, J.W., S.J. and J.G.; visualization, J.W. and J.G.; supervision, S.J. and G.Z.; project

administration, G.Z.; funding acquisition, S.J. and G.Z. All authors have read and agreed to the published version of the manuscript.

**Funding:** This research was funded by the fund of the Technology Innovation Center for the Monitoring and Restoration Engineering of the Ecological Fragile Zone in Southeast China, MNR (Grant NO. KY-090000-04-2021-006), and funded by the Project of Fujian Provincial Social Science Foundation (Grant NO. FJ2022B153).

**Data Availability Statement:** The data presented in this study are available on request from the corresponding author. The data are not publicly available due to the privacy requirement of the projects. The statistical data in this study can be found at <https://github.com/jsfzihuan> (accessed on 1 February 2023).

**Conflicts of Interest:** The authors declare no conflict of interest.

## References

- Cheng, W.-F.; Zhou, Y.; Wang, S.-X.; Han, Y.; Wang, F.-T.; Pu, Q.-Y. Study on the Method of Recognizing Abandoned Farmlands Based on Multispectral Remote Sensing. *Spectrosc. Spectr. Anal.* **2011**, *31*, 1615–1620.
- Xiong, Z.; Yao, Z.; Zhang, Y. Influential Factors of cropland abandonment Using Combination Weight and SEM: From the Perspective of Farmers Individual Capital. *Econ. Geogr.* **2017**, *37*, 155–161.
- Yang, G.; Xu, W. Cultivated land abandoning and its governance: Literature review and research prospective. *J. China Agric. Univ.* **2015**, *20*, 279–288.
- Shi, T.; Li, X. Cropland abandonment in Europe and Its Enlightenment to China. *Geogr. Geo-Inf. Sci.* **2013**, *29*, 101–103.
- Shao, J.A.; Zhang, S.; Li, X. Farmland marginalization in the mountainous areas: Characteristics, influencing factors and policy implications. *Acta Geogr. Sin.* **2014**, *69*, 227–242. [[CrossRef](#)]
- Ge, L.; Gao, M.; Hu, Z.; Han, X. Reasons of cultivated land abandonment in mountainous area based on farmers perspective. *Chin. J. Agric. Resour. Reg. Plan.* **2012**, *33*, 42–46.
- Khanal, N.R.; Watanabe, T. Abandonment of Agricultural Land and Its Consequences. *Mt. Res. Dev.* **2006**, *26*, 32–40. [[CrossRef](#)]
- Yin, H.; Prishchepov, A.V.; Kuemmerle, T.; Bleyhl, B.; Buchner, J.; Radeloff, V.C. Mapping agricultural land abandonment from spatial and temporal segmentation of Landsat time series. *Remote Sens. Environ.* **2018**, *210*, 12–24. [[CrossRef](#)]
- Zhang, B.; Yang, Q.; Yan, Y.; Xue, M.; Su, K.; Zang, B. Characteristics and Reasons of Different Households Farming Abandonment Behavior in the Process of Rapid Urbanization Based on a Survey from 540 Households in 10 Counties of Chongqing Municipality. *Resour. Sci.* **2011**, *33*, 2047–2054.
- Potdar, M.B. Sorghum yield modelling based on crop growth parameters determined from visible and near-IR channel NOAA AVHRR data. *Int. J. Remote Sens.* **1993**, *14*, 895–905. [[CrossRef](#)]
- Anderson, K.; Gaston, K.J. Lightweight unmanned aerial vehicles will revolutionize spatial ecology. *Front. Ecol. Environ.* **2013**, *11*, 138–146. [[CrossRef](#)] [[PubMed](#)]
- Chere, Z.; Abegaz, A.; Tamene, L.; Abera, W. Modeling and mapping the spatiotemporal variation in agricultural drought based on a satellite-derived vegetation health index across the highlands of Ethiopia. *Model. Earth Syst. Environ.* **2022**, *8*, 4539–4552. [[CrossRef](#)]
- Zhang, T.; Zhang, F.; Huang, J.; Li, C.; Zhang, B. Spatial pattern evolution of abandoned arable land and its influencing factor in industrialized region. *Trans. Chin. Soc. Agric. Eng.* **2019**, *35*, 246–255.
- Chen, L.; Jia, J.; Wang, H. An overview of applying high resolution remote sensing to natural resources survey. *Remote Sens. Land Resour.* **2019**, *31*, 1–7.
- Doraiswamy, P.C.; Hatfield, J.L.; Jackson, T.J.; Akhmedov, B.; Prueger, J.; Stern, A. Crop condition and yield simulations using Landsat and MODIS. *Remote Sens. Environ.* **2004**, *92*, 548–559. [[CrossRef](#)]
- Dong, J.; Xiao, X.; Menarguez, M.A.; Zhang, G.; Qin, Y.; Thau, D.; Biradar, C.; Moore, B., III. Mapping paddy rice planting area in northeastern Asia with Landsat 8 images, phenology-based algorithm and Google Earth Engine. *Remote Sens. Environ.* **2016**, *185*, 142–154. [[CrossRef](#)]
- Smaliychuk, A.; Mueller, D.; Prishchepov, A.V.; Levers, C.; Kruhlov, I.; Kuemmerle, T. Recultivation of abandoned agricultural lands in Ukraine: Patterns and drivers. *Glob. Environ. Chang.-Hum. Policy Dimens.* **2016**, *38*, 70–81. [[CrossRef](#)]
- Gorelick, N.; Hancher, M.; Dixon, M.; Ilyushchenko, S.; Thau, D.; Moore, R. Google Earth Engine: Planetary-scale geospatial analysis for everyone. *Remote Sens. Environ.* **2017**, *202*, 18–27. [[CrossRef](#)]
- Walker, E.; Venturini, V. Land surface evapotranspiration estimation combining soil texture information and global reanalysis datasets in Google Earth Engine. *Remote Sens. Lett.* **2019**, *10*, 929–938. [[CrossRef](#)]
- Pan, X.; Wang, Z.; Gao, Y.; Dang, X.; Han, Y. Detailed and automated classification of land use/land cover using machine learning algorithms in Google Earth Engine. *Geocarto Int.* **2022**, *37*, 5415–5432. [[CrossRef](#)]
- Gandharum, L.; Hartono, D.M.; Karsidi, A.; Ahmad, M. Monitoring Urban Expansion and Loss of Agriculture on the North Coast of West Java Province, Indonesia, Using Google Earth Engine and Intensity Analysis. *Sci. World J.* **2022**, *2022*, 3123788. [[CrossRef](#)]

22. Khanal, N.; Uddin, K.; Matin, M.A.; Tenneson, K. Automatic Detection of Spatiotemporal Urban Expansion Patterns by Fusing OSM and Landsat Data in Kathmandu. *Remote Sens.* **2019**, *11*, 2296. [[CrossRef](#)]
23. Liu, C.; Huang, H.; Sun, F. A Pixel-Based Vegetation Greenness Trend Analysis over the Russian Tundra with All Available Landsat Data from 1984 to 2018. *Remote Sens.* **2021**, *13*, 4933. [[CrossRef](#)]
24. Huang, H.; Chen, Y.; Clinton, N.; Wang, J.; Wang, X.; Liu, C.; Gong, P.; Yang, J.; Bai, Y.; Zheng, Y.; et al. Mapping major land cover dynamics in Beijing using all Landsat images in Google Earth Engine. *Remote Sens. Environ.* **2017**, *202*, 166–176. [[CrossRef](#)]
25. Maure, E.D.R.; Ilyushchenko, S.; Terauchi, G. A Simple Procedure to Preprocess and Ingest Level-2 Ocean Color Data into Google Earth Engine. *Remote Sens.* **2022**, *14*, 4906. [[CrossRef](#)]
26. Bunting, E.L.; Munson, S.M.; Bradford, J.B. Assessing plant production responses to climate across water-limited regions using Google Earth Engine. *Remote Sens. Environ.* **2019**, *233*, 111397. [[CrossRef](#)]
27. Zeng, Z.; Estes, L.; Ziegler, A.D.; Chen, A.; Searchinger, T.; Hua, F.; Guan, K.; Jintrawet, A.; Wood, E.F. Highland cropland expansion and forest loss in Southeast Asia in the twenty-first century. *Nat. Geosci.* **2018**, *11*, 556–562. [[CrossRef](#)]
28. Burke, M.; Lobell, D.B. Satellite-based assessment of yield variation and its determinants in smallholder African systems. *Proc. Natl. Acad. Sci. USA* **2017**, *114*, 2189–2194. [[CrossRef](#)]
29. Tuckett, P.A.; Ely, J.C.; Sole, A.J.; Livingstone, S.J.; Davison, B.J.; van Wessem, J.M.; Howard, J. Rapid accelerations of Antarctic Peninsula outlet glaciers driven by surface melt. *Nat. Commun.* **2019**, *10*, 4311. [[CrossRef](#)] [[PubMed](#)]
30. Wang, L.; Guo, Y.; He, J.; Liu, T.; Zhang, H.; Cheng, Y.; Yang, X.; Qin, F.; Wang, L. Approach for winter wheat yield estimation with remote sensing image at field scale. *J. China Agric. Resour. Reg. Plan.* **2021**, *42*, 243–253.
31. Yang, Y.; Wu, Z.; Luo, J.; Huang, Q.; Zhang, D.; Wu, T.; Sun, Y.; Cao, Z.; Dong, W.; Liu, W. Parcel-based crop distribution extraction using the spatiotemporal collaboration of remote sensing data. *Trans. Chin. Soc. Agric. Eng.* **2021**, *37*, 166–174.
32. Ni, G. Vegetation Index and Its Advances. *Arid. Meteorol.* **2003**, *4*, 71–75.
33. Cai, Z.; Bao, N.; Liu, S. Estimation Method of Fractional Vegetation Coverage for Grassland Based on Chinese GF-1 Satellite Image: Taking Hulun Buir Prairie Open-Pit Coal Mine as an Example. *Geogr. Geo-Inf. Sci.* **2017**, *33*, 32–38+44.
34. Hou, Q.; Wang, F.; Yan, L. Extraction of color image texture feature based on gray-level co-occurrence matrix. *Remote Sens. Land Resour.* **2013**, *25*, 26–32.
35. Jobanputra, R.; Clausi, D.A. Preserving boundaries for image texture segmentation using grey level co-occurring probabilities. *Pattern Recognit.* **2006**, *39*, 234–245. [[CrossRef](#)]
36. Liu, L.; Kuang, G.Y. Overview of Image Textural Feature Extraction Methods. *J. Image Graph.* **2009**, *14*, 622–635.
37. Haralick, R.M.; Shanmugam, K.; Dinstein, I. Textural Features for Image Classification. *Stud. Media Commun.* **1973**, *SMC-3*, 610–621. [[CrossRef](#)]
38. Connors, R.W.; Trivedi, M.M.; Harlow, C.A. Segmentation of a high-resolution urban scene using texture operators. *Comput. Vis. Graph. Image Process.* **1984**, *25*, 273–310. [[CrossRef](#)]
39. Breiman, L. Random forests, machine learning 45. *J. Clin. Microbiol.* **2001**, *2*, 199–228.
40. Parente, L.; Ferreira, L.; Faria, A.; Nogueira, S.; Araujo, F.; Teixeira, L.; Hagen, S. Monitoring the brazilian pasturelands: A new mapping approach based on the landsat 8 spectral and temporal domains. *Int. J. Appl. Earth Obs. Geoinf.* **2017**, *62*, 135–143. [[CrossRef](#)]
41. Wang, M.; Liu, P.; Chen, X.; Wang, F.; Song, Y.; Liu, H. Land Expansion of Urban Construction in the Three Provinces of Northeast China Based on Google Earth Engine. *J. Jilin Univ. Earth Sci. Ed.* **2022**, *52*, 292–304.
42. Li, J.; Ding, W.; Wang, B.; Nie, X.; Cui, C. An evaluation method for the influence of folk sports on body indicators based on random forest. *J. Nanjing Univ. Nat. Sci.* **2021**, *57*, 59–67.
43. Kennedy, R.E.; Yang, Z.; Cohen, W.B. Detecting trends in forest disturbance and recovery using yearly Landsat time series: 1. LandTrendr—Temporal segmentation algorithms. *Remote Sens. Environ.* **2010**, *114*, 2897–2910. [[CrossRef](#)]
44. Kennedy, R.E.; Yang, Z.; Gorelick, N.; Braaten, J.; Cavalcante, L.; Cohen, W.B.; Healey, S. Implementation of the LandTrendr Algorithm on Google Earth Engine. *Remote Sens.* **2018**, *10*, 691. [[CrossRef](#)]
45. Luo, Y.; Gong, J.; Li, T.; Hu, Y. Extraction of abandoned farmland based on MaxEnt model: A case study of Wusheng County, Sichuan Province. *J. Agric. Resour. Environ.* **2021**, *38*, 1084–1093.
46. Zhou, D.; Wu, J.; Wen, W.; Jiang, G.; Li, Y.; Li, G. Abandonment Characteristics and Influencing Factors of Cultivated Land Abandonment in Major Crop-producing Areas. *Trans. Chin. Soc. Agric. Mach.* **2021**, *52*, 127–137.
47. Liu, C.; Nie, W.; Zhao, X.; Shen, W. Regional differences and influencing factors in the contracted land use patterns for rural migrant workers: A perspective of social inclusion. *J. Nat. Resour.* **2022**, *37*, 424–439. [[CrossRef](#)]
48. Zhu, X.; Xiao, G.; Zhang, D.; Guo, L. Mapping abandoned farmland in China using time series MODIS NDVI. *Sci. Total Environ.* **2021**, *755*, 142651. [[CrossRef](#)]
49. Wu, M.; Hu, Y.; Wang, H.; Liu, G.; Yang, L. Remote sensing extraction and feature analysis of abandoned farmland in hilly and mountainous areas: A case study of Xingning, Guangdong. *Remote Sens. Appl.-Soc. Environ.* **2020**, *20*, 100403.
50. Wang, L.; Chen, Q.; Wu, Y.; Zhou, Z.; Dan, Y. Accurate recognition and extraction of karst abandoned land features based on cultivated land parcels and time series NDVI. *Remote Sens. Land Resour.* **2020**, *32*, 23–31.
51. Yusoff, N.M.; Muhamram, F.M. The Use of Multi-Temporal Landsat Imageries in Detecting Seasonal Crop Abandonment. *Remote Sens.* **2015**, *7*, 11974–11991. [[CrossRef](#)]

52. Hussain, M.; Chen, D.; Cheng, A.; Wei, H.; Stanley, D. Change detection from remotely sensed images: From pixel-based to object-based approaches. *ISPRS J. Photogramm. Remote Sens.* **2013**, *80*, 91–106. [[CrossRef](#)]
53. Yoon, H.; Kim, S. Detecting abandoned farmland using harmonic analysis and machine learning. *ISPRS J. Photogramm. Remote Sens.* **2020**, *166*, 201–212. [[CrossRef](#)]
54. Wang, H.; Wang, X.; Gao, L.; Li, Q.; Zhao, L.; Du, X.; Zhang, Y. Study on Extraction Method of Abandoned Farmland based on the Seasonal Variation Characteristics of Remotely Sensed Images. *Remote Sens. Technol. Appl.* **2020**, *35*, 596–605.
55. Morell-Monzo, S.; Estornell, J.; Sebastia-Frasquet, M.-T. Comparison of Sentinel-2 and High-Resolution Imagery for Mapping Land Abandonment in Fragmented Areas. *Remote Sens.* **2020**, *12*, 2062. [[CrossRef](#)]
56. Tiezhou, S. Research progress of cropland abandonment process and influence factors at home and abroad. *Hubei Agric. Sci.* **2020**, *59*, 11–16.
57. Prishchepov, A.V.; Mueller, D.; Dubinin, M.; Baumann, M.; Radeloff, V.C. Determinants of agricultural land abandonment in post-Soviet European Russia. *Land Use Policy* **2013**, *30*, 873–884. [[CrossRef](#)]
58. Benayas, R. Abandonment of agricultural land: An overview of drivers and consequences. *Cab Rev. Perspect. Agric. Vet. Sci. Nutr. Nat. Resour.* **2007**, *2*, 1–14. [[CrossRef](#)]
59. Gellrich, M.; Zimmermann, N.E. Investigating the regional-scale pattern of agricultural land abandonment in the Swiss mountains: A spatial statistical modelling approach. *Landsc. Urban Plan.* **2007**, *79*, 65–76. [[CrossRef](#)]
60. Aide, T.M. ECOLOGY: Enhanced: Globalization, Migration, and Latin American Ecosystems. *Science* **2004**, *305*, 1915–1916. [[CrossRef](#)]
61. Witmer, F.D.W. Detecting war-induced abandoned agricultural land in northeast Bosnia using multispectral, multitemporal Landsat TM imagery. *Int. J. Remote Sens.* **2008**, *29*, 3805–3831. [[CrossRef](#)]

**Disclaimer/Publisher’s Note:** The statements, opinions and data contained in all publications are solely those of the individual author(s) and contributor(s) and not of MDPI and/or the editor(s). MDPI and/or the editor(s) disclaim responsibility for any injury to people or property resulting from any ideas, methods, instructions or products referred to in the content.